# BRCA1 and CtIP suppress long tract gene conversion between sister chromatids

Published in final edited form as:
*Nat Commun*. 2013 ; 4: . doi:10.1038/ncomms3404.

# BRCA1 and CtIP suppress long tract gene conversion between sister chromatids

**Gurushankar Chandramouly**[1], **Amy Kwok**[1,2], **Bin Huang**[1], **Nicholas A. Willis**[1], **Anyong Xie**[1], and **Ralph Scully**[1,3]

[1]Beth Israel Deaconess Medical Center and Harvard Medical School, 330 Brookline Ave, Boston, MA 02215

## Abstract

BRCA1 controls early steps of the synthesis-dependent strand annealing (SDSA) pathway of homologous recombination, but has no known role following Rad51-mediated synapsis. Here we show that BRCA1 influences post-synaptic homologous recombination events, controlling the balance between short- (STGC) and long-tract gene conversion (LTGC) between sister chromatids. *Brca1* mutant cells reveal a bias towards LTGC that is corrected by expression of wild type but not cancer-predisposing *BRCA1* alleles. The LTGC bias is enhanced by depletion of CtIP but reversed by inhibition of 53BP1, implicating DNA end resection as a contributor to the STGC/LTGC balance. The impact of BRCA1/CtIP loss on the STGC/LTGC balance is abolished when the second (non-invading) end of the break is unable to support termination of STGC by homologous pairing ("annealing"). This suggests that BRCA1/CtIP-mediated processing of the second end of the break controls the annealing step that normally terminates SDSA, thereby suppressing the error-prone LTGC outcome.

## Introduction

Double-strand breaks (DSBs) are dangerous DNA lesions, the misrepair of which can promote genomic instability and cancer [1,2]. Chromosome breakage in proliferating cells commonly arises in the S phase of the cell cycle during replication across a damaged DNA template [3–5]. Such DSBs can be repaired by sister chromatid recombination (SCR), a potentially error-free pathway in which the broken chromosome uses the neighboring sister chromatid as a template for repair by homologous recombination (HR). The major hereditary breast/ovarian cancer predisposition genes, *BRCA1* and *BRCA2*, have established functions in HR. A long-standing hypothesis proposes that BRCA1 and BRCA2 execute tumor suppressor functions in sister chromatid recombination [6].

HR entails resection of the DNA end to single stranded (ss) DNA, on which Rad51 polymerizes to form a Rad51-ssDNA nucleoprotein filament [7–9]. This filament conducts a homology search by invading neighboring DNA duplexes and base-pairing with a homologous donor such as the neighboring sister chromatid. A DNA polymerase extends the invading 3' DNA end (the "nascent" strand). In somatic eukaryotic cells, the major HR

[3]Corresponding author: rscully@bidmc.harvard.edu.
[2]Current address: University of Massachusetts Medical School, 55 Lake Avenue North Worcester, MA 01655

Author contributions
G.C., A.K., B.H., N.A.W. and A.X performed the experiments. G.C. and R.S. designed the new HR reporters. G.C., N.A.W. and R.S. wrote the paper.

Competing Financial Interests
The authors declare that they have no competing financial interests.

pathway is "synthesis-dependent strand annealing" (SDSA), a non-crossover pathway in which termination occurs by annealing of the displaced nascent strand with complementary sequences in the resected second end of the broken chromosome [7]. Gene conversion can occur if the homologous donor differs in sequence from the broken chromosome.

Studies in yeast indicate the existence of at least two distinct copying mechanisms in HR, which differ in their fidelity. In *Saccharomyces cerevisiae*, the majority of somatic gene conversions entail SDSA-mediated copying of a short (< 200 bp) stretch of information from the donor. An alternative pathway termed break-induced replication (BIR) can mediate long gene conversions in yeast, potentially extending the nascent strand as far as the end of the chromosome [10–13]. BIR may entail formation of a *bona fide* replication fork at the site of recombination and therefore requires both leading and lagging strand synthesis. In yeast, BIR can arise in response to one-ended invasions occurring without a homologous second end, a key trigger being the failure of the second end of the DSB to effect termination of HR [14–17]. To what extent BIR operates in mammalian cells is not well understood.

In mammalian cells, gene conversions typically extend less than 100 bp ("short tract" gene conversion – STGC) [18–20]. A small proportion of HR events entail "long tract" gene conversion (LTGC), in which nascent strand synthesis extends several kilobases prior to termination [21–23]. LTGC is an error-prone HR outcome, causing tandem gene duplication and, rarely, multi-copy gene amplification [22]. Mammalian cells lacking any one of the *Rad51* paralogs *XRCC3, Rad51C* or *XRCC2* reveal a specific defect in STGC and marked bias in favor of LTGC, which accounts for ~25% of all gene conversions in *Rad51* paralog-deficient cells [23–25]. Increased proportions of LTGC-type products were also observed in a *Brca2* mutant hamster cell line and in *Nbs1* null chicken DT40 lymphoblastoid cells [26,27]. The identity of other genes that regulate the balance between STGC and LTGC is unknown.

BRCA1 supports DNA end resection via its interactions with CtIP (C-terminus-binding protein of adenovirus E1A-interacting protein) and the Mre11/Rad50/NBS1 (MRN) complex to generate ssDNA that serves as substrate for BRCA2-mediated Rad51 nucleoprotein filament formation [28]. BRCA1 also interacts with BRCA2 via the bridging protein, PALB2 (partner and localizer of BRCA2), as well as with BACH1/BRIP1 and the chromatin-associated RAP80 complex [29–32]. Deletion of *53bp1*, a gene implicated in NHEJ and in the suppression of DNA end resection, rescues the *Brca1* mutant phenotype in the mouse, suggesting a primary role for BRCA1 in DNA end resection [33]. Thus, the known functions of BRCA1 in HR are restricted to early steps preceding Rad51-mediated synapsis.

To test whether BRCA1 influences later HR steps, we studied its contribution to STGC and LTGC between sister chromatids, induced by a site-specific chromosomal DSB. We show here that loss of BRCA1 or CtIP skews HR in favor of the LTGC outcome; this is reversed by wild type *BRCA1* but not by certain cancer-predisposing *BRCA1* alleles. The influence of BRCA1 and CtIP on the STGC/LTGC balance is lost when the second (non-invading) end of the DSB is unable to support termination of STGC by annealing. We conclude that BRCA1/CtIP controls the balance between STGC and LTGC by acting on the second end of the DSB to support the annealing step that normally terminates STGC. These findings suggest that a defect in early stages of HR, caused by loss of BRCA1 function, can translate into a defect in HR termination, skewing this process towards error-prone repair at the expense of error-free repair.

## Results

### A reporter for rapid flow cytometric analysis of LTGC

We previously described a SCR reporter to simultaneously measure STGC and LTGC between sister chromatids [22,34]. Expression of the rare-cutting homing endonuclease I-SceI [35] induces a site-specific DSB within a mutant copy of the gene encoding enhanced Green Fluorescent Protein (E-GFP, here termed "GFP"). Recombination between the broken *GFP* copy and neighboring 5' truncated *GFP* sequences produces wild type *GFP* by gene conversion, and the cell changes from $GFP^-$ to $GFP^+$. In the original reporter, duplication of a cassette during LTGC enabled positive selection of LTGC through expression of a wild type antibiotic resistance gene [22]. We re-fashioned this reporter so that the cassette duplicated during LTGC encodes the monomeric Red Fluorescent Protein RFP1.3 (here termed "RFP"; Fig. 1A) [36]. Briefly, we divided the *RFP* cDNA into two artificial exons ("A" and "B" in Fig. 1A), with appropriate splice donor and acceptor sequences. The *RFP* exons were placed "head to toe" between the two *GFP* copies of the reporter so that transcription of exon A within the unmodified ("parental") reporter will not lead to expression of wild type *RFP*. During STGC, the cell becomes $GFP^+RFP^-$ (Fig. 1A, outcome #1). In contrast, LTGC typically generates three *GFP* copies ("*GFP* triplication") by SCR and duplicates the *RFP* cassette (Fig. 1A, outcome #2). Splicing between exon A of the first cassette and exon B of the second generates wt*RFP* mRNA and the cell becomes $GFP^+RFP^+$. A minority of LTGCs duplicate *RFP* exon B but terminate prior to triplication of the *GFP* copies ("early termination" of LTGC—nascent strand extension of between 1252 bp and 3.4 kb).

We targeted a single copy of the RFP-SCR reporter to the *ROSA26* locus of the mouse embryonic stem (ES) cell line 11CO/47T [37], in which one *Brca1* allele is truncated and the second can be conditionally inactivated by Cre-mediated recombination (here termed "$Brca1^{fl/mut}$" cells, described in detail below; see Methods). Transfection of $Brca1^{fl/mut}$ RFP-SCR reporter cells with I-SceI elicited $GFP^+RFP^-$ and $GFP^+RFP^+$ products (Fig. 1B). We used fluorescence activated cell sorting (FACS) to sort single $GFP^+RFP^-$ or $GFP^+RFP^+$ cells from I-SceI-transfected samples, prepared genomic DNA (gDNA) from amplified clones and analyzed the structure of the RFP-SCR reporter by Southern blotting. All FACS-sorted $GFP^+RFP^-$ clones revealed a structurally unrearranged RFP-SCR reporter, consistent with STGC (examples in Fig. 1C, lanes G1-G3). In contrast, >95% of $GFP^+RFP^+$ clones revealed rearrangements of the RFP-SCR reporter characteristic of LTGC (examples in Fig. 1C, lanes T1-T3; more detailed mapping in Supplementary Fig. S1).

### Donor sister chromatid distinguishes LTGC from crossing over

The "*GFP* triplication" outcome could arise by either LTGC or crossing over. In LTGC, the donor sister chromatid is unaltered, whereas crossing over results in loss of one *GFP* copy from the donor sister (Fig. 1D). Previous work established that crossing over is suppressed in somatic cells [21,23]. To distinguish these mechanisms, we adapted a strategy we used previously to capture the donor sister chromatid in the context of I-SceI-induced HR [23]. We found that a small fraction of sorted I-SceI-induced $GFP^+RFP^+$ cells were mixed colonies, in which the $GFP^+RFP^+$ cell had been sorted subsequent to an LTGC event but prior to the ensuing mitosis. Such clones should therefore contain HR products from both sister chromatids. We identified four such mixed colonies; all (4/4) revealed the "*GFP* triplication" outcome and an unrearranged donor (for example, lane T3 in Fig. 1D). Although the number of events detected was small, the consistently unrearranged donor suggests that LTGC is the major mechanism underlying the "*GFP* triplication" outcome.

## Bias in favor of LTGC in *Brca1*$^{\Delta/mut}$ RFP-SCR reporter cells

Figure 2A depicts the structure of the two *Brca1* alleles in *Brca1*$^{fl/mut}$ ES cell line 11CO/47T [37]. One allele ("*Brca1*$^{mut}$") encodes a C-terminally truncated *Brca1* gene product (lacking a functional BRCT repeat). The second allele ("*Brca1*$^{fl}$") contains mouse *Brca1* cDNA sequences corresponding to exons 22–24 flanked by *loxP* sites (Fig. 2A). Cre-mediated deletion converts the functionally wt *Brca1*$^{fl}$ allele to a mutant allele ("*Brca1*$^{\Delta}$") that encodes a C-terminally truncated *Brca1* product similar to that encoded by the *Brca1*$^{mut}$ allele. We transduced *Brca1*$^{fl/mut}$ RFP-SCR reporter ES cells with Cre-encoding adenovirus and screened clones for *Brca1* inactivation by real time qPCR (Fig. 2B and Methods). We identified *Brca1*-deleted clones and others that remained undeleted. *Brca1* null ES cells are unviable [38]; very likely, *Brca1*$^{mut}$ *and Brca1*$^{\Delta}$ are hypomorphic alleles. Consistent with this, we detected by immunoblotting *Brca1* gene products at low abundance in *Brca1*$^{\Delta/mut}$ ES cells clones. These Brca1 proteins were further depleted by siRNA directed to *Brca1* (Fig. 2B).

To determine whether loss of wt*Brca1* influences the balance between STGC and LTGC, we transfected, in parallel, the above-noted Cre-treated *Brca1*$^{fl/mut}$ and *Brca1*$^{\Delta/mut}$ RFP-SCR reporter clones with either I-SceI plasmid or empty vector and quantified HR products (Fig. 2C; see Methods). In all experiments described here, clones that were treated with empty vector control revealed typical background levels of ~0.03% GFP$^{+}$RFP$^{-}$ and of <0.001% GFP$^{+}$RFP$^{+}$, with at least 200,000 events counted per sample. All I-SceI-induced HR measurements were corrected for background events and for I-SceI transfection efficiency (see Methods), the latter being typically between 65% and 85%; neither measurement varied with *Brca1* status. We compared four independent Cre-treated *Brca1*$^{\Delta/mut}$ and *Brca1*$^{fl/mut}$ RFP-SCR reporter clones. All four *Brca1*$^{\Delta/mut}$ clones revealed reduced frequencies of HR, as expected [39], but only a modest reduction in LTGC (Fig. 2C). The ratio: GFP$^{+}$RFP$^{+}$/Total GFP$^{+}$ estimates the probability that an I-SceI-induced GFP$^{+}$ HR event will resolve as LTGC. This probability was elevated ~2-fold in *Brca1*$^{\Delta/mut}$ cells in comparison with isogenic *Brca1*$^{fl/mut}$ cells (Fig. 2C, lower panel). Thus, loss of wt*Brca1* skews HR in favor of LTGC.

We studied the structure of the reporter in I-SceI-induced GFP$^{+}$RFP$^{+}$ clones derived from *Brca1*$^{\Delta/mut}$ cells and isogenic Cre-treated *Brca1*$^{fl/mut}$ cells by Southern blotting. As noted above, most LTGCs entail "*GFP* triplication" (Fig. 1A, outcome #2), while a minority terminate within the reporter subsequent to duplication of *RFP* exon B ("early termination") [21–23,34]. In *Brca1*$^{fl/mut}$ cells, 58/65 (89.2%) GFP$^{+}$RFP$^{+}$ clones entailed *GFP* triplication while 4/65 (6.1%) GFP$^{+}$RFP$^{+}$ clones revealed early termination of LTGC. In *Brca1*$^{\Delta/mut}$ cells, 28/29 (96.6%) of GFP$^{+}$RFP$^{+}$ clones were *GFP* triplications and 1/29 (3.4%) revealed early termination of LTGC. Thus, loss of *Brca1* does not grossly alter the types of LTGC detected. Capture and analysis of the donor sister chromatid in mixed I-SceI-induced GFP$^{+}$RFP$^{+}$ clones sorted from *Brca1*$^{\Delta/mut}$ cells revealed an intact donor sister chromatid in 3/3 *GFP* triplication clones examined, confirming that they arose by a non-crossover mechanism, i.e., by LTGC.

## Wild type *BRCA1* rescues the HR defects of *Brca1*$^{\Delta/mut}$ cells

The bias in favor of LTGC noted in *Brca1*$^{\Delta/mut}$ cells could reflect secondary/compensatory responses to *Brca1* loss. To test this, we transiently co-transfected *Brca1*$^{\Delta/mut}$ and, in parallel, *Brca1*$^{fl/mut}$ RFP-SCR reporter clones with wt human *BRCA1* and I-SceI and measured HR. Human *BRCA1* can restore normal development to *Brca1* null mice [40]. Notably, wild type *BRCA1* complemented the STGC defect and corrected the LTGC bias in *Brca1*$^{\Delta/mut}$ cells, but had little impact on any HR measurements in *Brca1*$^{fl/mut}$ cells (Fig. 3). In contrast to wt*BRCA1*, expression of cancer-predisposing *BRCA1* alleles encoding point

mutant products affecting the RING domain (C61G, C64G; Figs. 3A–3C) or the tandem BRCT repeat (P1749R, M1775R; Figs. 3D–3F) had no impact on HR in *Brca1*$^{\Delta/mut}$ cells, despite levels of *BRCA1* mutant gene expression higher than those of wt*BRCA1* (Supplementary Fig. S2; at the low levels of exogenous *BRCA1* used in these experiments, we were unable to detect the hBRCA1 protein). These results suggest that a tumor suppressor function of *BRCA1* specifically enforces STGC in favor of LTGC.

The above experiments implicate both the BRCA1 N-terminal RING and C-terminal BRCT domains in STGC and in preventing an LTGC bias during HR. The BRCA1 RING domain mediates constitutive heterodimerization with BARD1 in vertebrate cells and BRCA1 RING domain mutations C61G and C64G disrupt the BRCA1-BARD1 interaction, while retaining some residual function [41,42]. We used transient transfection of siRNA to deplete either Brca1 or Bard1 in *Brca1*$^{\Delta/mut}$ or *Brca1*$^{fl/mut}$ RFP-SCR reporter cells in conjunction with I-SceI transfection (see Methods). Consistent with the hypomorphic status of *Brca1*$^{\Delta/mut}$ cells, siRNA-mediated depletion of Brca1 reduced HR in both *Brca1*$^{\Delta/mut}$ and *Brca1*$^{fl/mut}$ cells (Supplementary Fig. S3). siRNA-mediated depletion of Brca1 also further exacerbated the LTGC bias in *Brca1*$^{\Delta/mut}$ cells, but produced only minimal alterations in the STGC/LTGC balance in *Brca1*$^{fl/mut}$ cells. A similar pattern was observed following siRNA-mediated depletion of Bard1 (Supplementary Fig. S3). The limited impact of *Brca1*-specific siRNA on the STGC/LTGC balance in *Brca1*$^{fl/mut}$ cells may reflect residual activity of wt*Brca1* in siRNA-depleted *Brca1*$^{fl/mut}$ cells, and indicates that siRNA-mediated methods for perturbing the LTGC/STGC balance have false negative rates, as was noted previously [23].

## CtIP regulates the balance between STGC and LTGC

At least three major distinct DNA damage response complexes interact with the BRCA1/BARD1 heterodimer via the BRCA1 tandem BRCT repeat, which they bind in a mutually exclusive fashion. These are (direct BRCA1-interactors underlined): CCDC98/Abraxas, RAP80, BRCC36, BRCC45, and MERIT40; BACH1 and TopBP1; and CtIP [29–31]. These interactions are disabled by BRCA1 BRCT mutations P1749R and M1775R. The failure of these BRCA1 BRCT mutants to restore a normal STGC/LTGC balance to *Brca1*$^{\Delta/mut}$ cells therefore suggested possible roles for CtIP, BACH1 or Abraxas/Rap80 as regulators of the STGC/LTGC balance. Bach1 depletion reduced HR in both *Brca1*$^{\Delta/mut}$ and *Brca1*$^{fl/mut}$ cells [43] (Supplementary Fig. S4). This suggests that at least part of Bach1's HR function is independent of its interaction with Brca1. Rap80 depletion caused an unexpected reduction in HR in both *Brca1*$^{\Delta/mut}$ and *Brca1*$^{fl/mut}$ cells, in contrast to recent findings of several groups in cells with normal BRCA1 function [32,44,45]. We do not understand the reason for this difference; however, Rap80 depletion was found to reduce HR in one other study, suggesting that Rap80's function in HR is context-dependent [46]. siRNA-mediated depletion of CtIP, using either a single siRNA or SMARTpool siRNAs of non-overlapping specificity with the single CtIP siRNA, reduced HR in both *Brca1*$^{\Delta/mut}$ and *Brca1*$^{fl/mut}$ cells—indicating that CtIP, like Bach1, can function in HR independent of its Brca1 interaction. siRNA-mediated depletion of BACH1 or Rap80 revealed exactly proportional alterations in I-SceI-induced STGC and LTGC in both *Brca1*$^{\Delta/mut}$ and *Brca1*$^{fl/mut}$ cells (Supplementary Fig. S4). In contrast, surprisingly, depletion of CtIP biased HR in favor of LTGC in both *Brca1*$^{\Delta/mut}$ and *Brca1*$^{fl/mut}$ cells (Figs. 4A – C).

CtIP regulates DNA end resection and is activated by the SIRT6 deacetylase [47]. Notably, Sirt6 depletion mimicked the effect of CtIP depletion, skewing HR in favor of LTGC, as did depletion of Exo1, an exonuclease implicated in DNA end resection (Fig. 5 and Supplementary Fig. S5); Inhibition of 53BP1—an antagonist of Brca1 DNA end resection function [33]—using a previously characterized dominant negative fragment of 53BP1 [48], specifically restored the STGC/LTGC balance to *Brca1*$^{\Delta/mut}$ cells but did not affect this balance in *Brca1*$^{fl/mut}$ cells (Fig. 5). This supports the idea that the LTGC bias in *Brca1*$^{\Delta/mut}$

cells is caused by a defect in DNA end resection. siRNA-mediated depletion of the early DSB response protein Mre11 had no impact on the STGC/LTGC balance, suggesting that not all resection proteins influence this balance (Supplementary Fig. S5). We considered the possibility that the LTGC bias in ES cells depleted of CtIP might reflect altered cell cycle distribution [49]. However, cell cycle distribution did not vary between *Brca1*$^{\Delta/mut}$ or *Brca1*$^{fl/mut}$ cells, whether they received siRNA directed to Luciferase, Bard1 or CtIP (Supplementary Fig. S6). We determined whether the LTGC bias in cells lacking BRCA1/BARD1/CtIP is unique to mouse ES cells by studying human U2OS osteosarcoma cells carrying a single integrated copy of the RFP-SCR reporter (see Methods). Consistent with the above results, we observed a bias towards LTGC in U2OS cells depleted of BRCA1, BARD1 or CtIP (Supplementary Fig. S7). Taken together, the results reveal a surprising and specific role for BRCA1/BARD1, CtIP and certain other DNA end resection complexes in controlling the balance between STGC and LTGC.

## Brca1/CtIP controls the annealing step of SDSA

The idea that a defect in DNA end resection could translate into a defect in late stages of HR seems paradoxical. We considered the hypothesis that the bias towards LTGC in *Brca1* mutant cells is the consequence of failed termination of STGC. We tested this hypothesis by constructing a new "one-ended" RFP-SCR reporter, in which the non-invading DNA end (marked with a red star in Fig. 6A) lacks *GFP* sequences. I-SceI-induced STGC ($GFP^+RFP^-$) occurring in this reporter cannot be terminated by homologous pairing (annealing), but must instead use non-homologous mechanisms to rejoin the displaced nascent strand with the non-invading, non-homologous second end of the DSB.

We targeted a single copy of the "one-ended" RFP-SCR reporter to the *ROSA26* locus of *Brca1*$^{fl/mut}$ ES cells. We generated isogenic clones of Cre-treated *Brca1*$^{fl/mut}$ one-ended RFP-SCR reporter cells that either had or had not undergone deletion of wt*Brca1*. Consistent with the longer gene conversion (332 bp) required to produce $GFP^+$ products, we noted ~10-fold lower frequencies of I-SceI-induced STGC ($GFP^+RFP^+$) products in *Brca1*$^{fl/mut}$ cells compared to isogenic *Brca1*$^{fl/mut}$ cells containing a conventional "two-ended" RFP-SCR reporter (Fig. 6B); in contrast, the absolute frequencies of I-SceI-induced LTGC were little changed (Fig. 6B). Typically, about one third of all measured HR products were $GFP^+RFP^+$, the remainder being $GFP^+RFP^-$; this varied from clone to clone, the maximum LTGC:total HR ratio being ~60%. Southern analysis of FACS-sorted I-SceI-induced $GFP^+RFP^-$ or $GFP^+RFP^+$ populations derived from either *Brca1*$^{fl/mut}$ or from *Brca1*$^{\Delta/mut}$ cells revealed STGC products of variable size, reflecting random termination by end joining (Fig. 6C); LTGC products revealed a combination of "early terminating" LTGC (i.e., LTGC with termination occurring between the two *GFP* copies of the donor) and "*GFP* triplications" (Fig. 6C). Consistent with the absence of an annealing step that can reliably terminate STGC, we noted a higher proportion of "early terminating" LTGCs in one-ended reporter cells than in the original two-ended reporter cells: in *Brca1*$^{fl/mut}$ one-ended RFP-SCR reporter cells, 6/21 (29%) of all LTGCs were early terminating and 15/21 (71%) were *GFP* triplications; in *Brca1*$^{\Delta/mut}$ one-ended RFP-SCR reporter cells, 9/23 (39%) of all LTGCs were early terminating and 14/23 (61%) were *GFP* triplications (difference between *Brca1*$^{fl/mut}$ and *Brca1*$^{\Delta/mut}$is not significant by $x^2$ analysis).

We noted reduced I-SceI-induced HR frequencies in four independent one-ended RFP-SCR reporter *Brca1*$^{\Delta/mut}$ clones, in comparison with four independent *Brca1*$^{fl/mut}$ clones (Fig. 7A). However, HR in *Brca1*$^{\Delta/mut}$ one-ended RFP-SCR reporter cells revealed exactly proportionate reductions in STGC and LTGC, with no additional LTGC bias (Fig. 7A). Further, transient expression of wt*BRCA1* in *Brca1*$^{\Delta/mut}$ one-ended RFP-SCR reporter cells restored both STGC and LTGC in equal proportions (Fig. 7B). Thus, in contrast to the conventional two-ended RFP-SCR reporter (Fig. 3), in the context of the one-ended RFP-

SCR reporter, STGC and LTGC are each equivalently *Brca1*-dependent (Fig. 7B). Further, siRNA-mediated depletion of CtIP reduced STGC and LTGC in equal proportions in both *Brca1*$^{fl/mut}$ and *Brca1*$^{\Delta/mut}$ one-ended RFP-SCR reporter cells and thus had no statistically significant impact on the STGC/LTGC balance (Fig. 7C). Therefore, when the annealing step of STGC is inactivated, loss of Brca1/CtIP has no impact on the relative balance between STGC and LTGC.

## Discussion

This report documents a functional communication between BRCA1 and later stages of HR, as revealed by a bias towards LTGC when BRCA1 function is impaired. Expression of wild type but not cancer-predisposing *BRCA1* alleles restored the STGC/LTGC balance in *Brca1* mutant cells, suggesting that *BRCA1* performs a tumor suppressor function in this process. Depletion of the BRCA1-interacting end resection protein CtIP (or its activator, Sirt6) or of Exo1 mimicked or enhanced the *Brca1* mutant STGC/LTGC imbalance. Further, inhibition of 53BP1, a key antagonist of the DNA end resection function of Brca1, normalized the STGC/LTGC balance in *Brca1*$^{\Delta/mut}$ cells. This suggests that defects in DNA end processing are the cause of the LTGC bias in *Brca1*$^{\Delta/mut}$ cells. To identify mechanisms underlying this phenomenon, we studied STGC and LTGC within a new “one-ended” reporter, in which STGC cannot be terminated by annealing. Surprisingly, in the context of the “one-ended” reporter, although overall HR retained dependence on BRCA1 and CtIP, loss of BRCA1/CtIP no longer influenced the balance between STGC and LTGC. This suggests that BRCA1/CtIP influences the STGC/LTGC balance in the context of two-ended DSBs by facilitating the annealing step that normally terminates STGC—most likely, by ensuring efficient and timely processing of the second end of the DSB (Fig. 8).

The SDSA model of somatic HR assumes an asymmetry between the two DNA ends, such that one end undergoes Rad51-mediated strand exchange and the second end does not (Fig. 8) [7]. How asymmetry is established during SDSA is unknown; it could be imposed at several different stages, including the DNA end resection stage or during Rad51 filament assembly. Although the model proposed in Fig. 8 envisions a direct role for Brca1, CtIP and Exo1 in resection of the non-invading second end of the DSB, one or more of these proteins might also coordinate communication between the two DNA ends during end resection. Interestingly, Recent work in *S. cerevisiae* shows that the Mre11 nuclease and the CtIP homolog, Sae2, provide coordinated resection of the two ends of radiation-induced DSBs [50]. Currently, however, it is not possible to measure second end resection or potential asymmetry between the two DNA ends in mammalian cells. Interestingly, the failure of Mre11 depletion to influence the STGC/LTGC balance suggests that not all mammalian complexes implicated in DNA end resection affect the balance between STGC and LTGC. In this regard, deletion of *H2AX*, an HR gene that can suppress DNA end resection in certain contexts [51], does not appear to influence the STGC/LTGC balance [34].

Analyses of the impact of *POL32* mutation on gap repair in *S. cerevisiae* [52] and in Drosophila melanogaster [53] suggest that SDSA may entail several different mechanisms of nascent strand extension that differ in their processivity and, hence, in their capacity to mediate LTGC. A major alternative model proposes that mammalian LTGC is mediated by a distinct copying mechanism, such as break-induced replication (BIR). BIR may entail formation of a *bona fide* replication fork following strand exchange and therefore involves lagging strand synthesis [11,15,54]. A key trigger to BIR in yeast is a one-ended invasion occurring without a homologous second end [10,11,14–17]. In yeast, both *RAD51*-independent and *RAD51*-dependent forms of BIR are recognized [7,11,14,15 13] *RAD51*-independent BIR can act on short homologous sequences, tolerating homologies down to ~30 bp [55]. By analogy, a defect in DNA end resection and Rad51 loading in *Brca1* mutants might lead to

the formation of abnormal synapses that favor BIR—perhaps similar to the recently proposed idea of microhomology-mediated BIR (MM-BIR) [56]—leading to the observed LTGC bias in *Brca1* mutants. We consider this BIR model of LTGC in detail below.

In contrast to the avid engagement of BIR following chromosomal one-ended invasions in *S. cerevisiae*, the majority of chromsomal one-ended HR events in the mammalian system studied here resolve as STGCs, as revealed by the abundance of $GFP^+RFP^-$products in this setting. There is indeed a *proportionate* bias in favor of LTGC in the "one-ended" reporter compared to the "two-ended" reporter; however, the absolute frequencies of I-SceI-induced LTGC at the *ROSA26* locus in $Brca1^{fl/mut}$ cells are equal in the two reporters (~0.05%; compare LTGC frequencies in Figs. 2C and 7A). Thus, a forced "one-ended" invasion in mammalian cells does not preferentially trigger BIR. The major effect of a forced "one-ended" invasion in our experiments is a ~10-fold reduction in the frequency of $GFP^+RFP^-$ STGCs (compare STGC frequencies in Figs. 2C and 7A). Importantly, a gene conversion of at least 331 bp is required to generate $GFP^+$ recombinants within the "one-ended" reporter. The Jasin and Nickoloff labs previously measured gene conversions (GCs) within a conventional "two-ended" reporter in mammalian cells and observed that ~80% of all GCs are less than 58bp in length [19,20]. This suggests that the majority of STGCs occuring within the "one-ended" reporter studied here may have been terminated prior to conversion to wt*GFP* and are therefore not detectable as $GFP^+$ products. Our findings are consistent with DNA fiber analysis of mammalian cells recovering from replication arrest, in which Rad51-dependent HR repair of collapsed forks—presumably mediated by one-ended invasions—was not found to be associated with replication restart [57].

Importantly, a pure 'replication fork' BIR model of LTGC also fails to explain why LTGC should be relatively independent of BRCA1 in the "two-ended" reporter (Figs. 2 and 3), but fully BRCA1-dependent in the context of the "one-ended" reporter (Figs. 7A and 7B). In contrast, an SDSA model of LTGC can readily account for this difference, since it invokes a defect of HR initiation in *Brca1* mutant cells and, for the "two-ended" reporter only, a defect of STGC termination by annealing (Fig. 8). These two defects will have opposing effects on the absolute frequency of LTGC only in the context of the "two-ended" reporter and might create the appearance that LTGC is *BRCA1*-independent in this setting (as in Fig. 3). Notably, Rad51-mediated invasions can trigger BIR in *Xenopus laevis* egg extracts [58] and it seems likely that a proportion of LTGCs in mammalian cells are *bona fide* BIR products. However, definitive analysis must await the development of an assay in mammalian cells that reliably separates BIR-mediated LTGCs from SDSA-mediated LTGCs.

A defect in annealing suggests a new mechanism underlying genomic instability associated with loss of BRCA1. In *BRCA1* mutant cells, a higher proportion of HR events may escape the error-free annealing step of SDSA termination; these "functionally one-ended" invasions will be obligatorily mutagenic. Thus, the *BRCA1*-dependent annealing step of SDSA termination is likely an important bulwark against genomic instability and cancer. Interestingly, a recent sequencing analysis of breast cancer genomes revealed elevated frequencies of tandem gene segment duplications [59]. Conceivably, some of these rearrangements could be the result of inappropriate engagement of LTGC during DSB repair.

## Methods

### Molecular biology and antibodies

The RFP-SCR reporter was constructed by conventional cloning methods using modified *ROSA26* targeting vectors [34]. Expression vector for h*BRCA1* was pcDNA3β [60]. siRNA SMARTpools were purchased from Dharmacon. Antibodies used were: Brca1 (Santa Cruz

and anti-human BRCA1 Ab MS110, 1:100), CtIP (Santacruz,1:50), Bard1 (Santacruz, 1:500), Mre11 (Novus, 1:6000), Sirt6 (Abcam, 1:500), Exo1 (Santacruz, 1:500), beta-actin (Abcam, 1:2000) and influenza hemagglutinin epitope tag Ab (Santacruz, 1:1000). Cells were lysed in RIPA buffer (50mM Tris-Hcl, pH 8.0, 250 mM NaCl, 0.1% sodium dodecyl sulfate, 1% NP-40 with protease and phosphatase inhibitors. Extracted protein was resolved by 4 −12 % bis-Tris SDS-PAGE (Invitrogen) and analyzed by Western blotting using the antibodies described above. Supplementary Figs. S8 – S15 show full gel images of western blots and of one Southern blot shown in other figures.

### Cell Lines and Cell Culture

Brca1fl/mut ES cell line (11CO/47T) was a kind gift from Dr. Alan Ashworth [37]. ES cells were grown in ES medium on either MEF feeders or gelatinized plates. The RFP-SCR reporter was targeted by electroporating $2 \times 10^7$ *Brca1*$^{fl/mut}$ ES cells with 20 μg of linearized targeting vector, followed by seeding in 60 cm plates with puroR feeders. Puromycin (0.5 μg/ml) was added 24 hours later and colonies were picked 5–7 days later. *Brca1*$^{fl/mut}$ ES cells contain one mutant *Brca1* allele encoding a truncated gene product and a second *Brca1* allele (which is functionally wild type but harbors *loxP* sites flanking exons 22–24) that can be conditionally inactivated by Cre-mediated recombination. We generated multiple *Brca1* deficient ES clones by transient adenovirus-mediated Cre expression to delete the exons 22–24. Cell line U2OS was obtained from ATCC.

### Southern Blotting

gDNA was extracted from confluent ES cells on 6-well plates (5–10 × 106 cells) using a Puregene DNA Isolation Kit (Gentra Systems). Southern blotting was performed with *GFP* cDNA or *ROSA26* 5' probe. 7.5–10 μg of genomic DNA was digested with appropriate restriction enzyme and run overnight on 0.8% gel with 0.5x TBE at 35V. The DNA was transferred overnight onto nylon membrane in 1M NaCl, 0.4M NaOH. The membrane was prehybridized for 30 minutes and labeled with *GFP* cDNA or *ROSA26* 5' probe overnight [34]. The membrane was then washed and developed by autoradiography. In all experiments, including U2OS cells containing a randomly integrated reporter, only clones containing one intact copy of the reporter were used. Supplementary Fig. S8 – S15 show full gel images of western blots and of one Southern blot shown in other figures.

### Recombination Assays

$2 \times 10^5$ cells were transfected in suspension in 24-well plates with 0.5 μg pcDNA3β–myc NLS-I-SceI [22] or 0.5 μg control vector pcDNA3β using Lipofectamine 2000 (Invitrogen). $GFP^+$ and $GFP^+RFP^+$ frequencies were measured 3 days post transfection by FACS using Becton Dickinson 5 Laser LSRII in triplicates and corrected for transfection efficiency and background events. (Transfection efficiency was measured simultaneously by parallel transfection with 0.05 μg wt *GFP* expression vector.) Typically ~$2 \times 10^5$ total events were scored per sample. In the *BRCA1* complementation experiments (Figure 3), rescue was optimal at low levels of exogenous *BRCA1* expression vector (0.1 μg pcDNA3β–*BRCA1* + 0.4 μg pcDNA3β–myc NLS-I-SceI or control vector per well). For siRNA experiments, cells were transfected with 1 μl 20μM (i.e., 20 pmol) siRNA + 0.3 μg of pcDNA3β–myc NLS-I-SceI (or control vector) per well. In Figures 3, 4, 5 and 6, HR data represents the mean and standard error of the mean of three independent experiments. Statistical analysis was by two-tailed paired t-test (unknown variance).

### RT-qPCR analysis

RNA was extracted using QIAGEN RNeasy Mini Kit (QIAGEN Sciences, Maryland, MD). Analysis of first-strand cDNA was by Power SYBR Green RNA-to$C_T$™ 1-Step Kit

(Applied Biosystems, Foster City, CA). An ABI 7300 Real time PCR System was used for RT-qPCR. Taqman probe and primer sets to genotype for *Brca1* were: *Brca1*-Exon-22-23-sense-TTC CGT GGT GAA GGA GCT T; *Brca1*-Exon-22-23-antisense-TGG CTG CAC GAT CAC AAC; *Brca1*-Exon-23-24-sense-GCC TGG ACA GAA GAC AGC A; *Brca1*-Exon-23-24-antisense-CAG TCC CAC ATC ACA AGA CG. We used conventional SYBR green RT-qPCR assays of *Gapdh* and siRNA-targeted gene. We used Primer 3 software (Whitehead Institute, MIT) to generate gene-specific primer sequences confirmed use of each primer pair by melting curve analysis and gel electrophoresis. Primers for RT-PCR: Human *BRCA1*-sense-TCA CAT GAT GGG GAG TCT GA; Human *BRCA1*-antisense-TTC CCG ATA GGT TTT CCC AAA; *Brca1*-EXON21-22-sense-ATG AGC TGG AGA GGA TGC TG; *Brca1*-EXON21-22-antisense-CTG GGC AGT TGC TGT CTT CT; *Brca1*-EXON22-23-sense-GGT GCT CAT CTA GTT GTG ATC G; *Brca1*-EXON22-23-antisense-CTG TAC CAG GTA GGC ATC CA; *Brca1*-EXON7-8-sense-AGC CTA GGT GTC CAG CTG TC; *Brca1*-EXON7-8-antisense-CTG CAA TCA CCT GGC TTA GTT; *CtIP*-sense-ATG GTC AAG AAT CTG AAC CC; *CtIP*-antisense-TGA GGA GGT GTC TTT GAA GCA G; *Bach1*-sense-ATC CGG TGT CAG AGA TGT CC; *Bach1*-antisense-CAA GGA GTA GAG CCC GTG AG; *Rap80*-sense-GAA GGA AAA CCC TCC TCC TG; *Rap80*-antisense-TGT TCT TGG CCT CTC TTC GT. *mRNA* was measured in triplicates with a standard curve generated for each gene using cDNA obtained from each sample. The expression level of target genes was normalized to internal *Gapdh*.

### Cell cycle analysis

ES cells were pulsed with 10 μM BrdU for 15 minutes, 48 hours after transfection with siRNA, and fixed in 70% ethanol. BrdU was counterstained using anti-BrdU (Boehringer-Mannheim, 1:40) with a secondary FITC-conjugated rabbit anti-mouse antibody (Jackson Immuno Research, 1:50). After exposure to RNase and staining with propidium diiodide, approximately $10^4$ events were acquired using a Becton Dickinson 5 Laser LSR II and the results were analyzed using FloJo software.

## Supplementary Material

Refer to Web version on PubMed Central for supplementary material.

## Acknowledgments

We thank Dr. Alan Ashworth for the *Brca1*$^{fl/mut}$ ES cell line and Drs. Richard Baer and Jagesh Shah for plasmids and antibodies. We thank Drs. Michael Resnick and Anna Malkova for communicating the results of unpublished experiments, Drs. Jim Haber, Lorraine Symington and Steve Jackson, as well as members of the Scully lab for valuable comments and critique. This work was supported by NIH grants CA095175 and GM073894 (to R.S.), T32 Training Grant in Cancer Biology CA081156 and an ACS postdoctoral fellowship (to N.A.W.).

## References

1. Ciccia A, Elledge SJ. The DNA damage response: making it safe to play with knives. Mol Cell. 2010; 40:179–204. [PubMed: 20965415]
2. Hartlerode AJ, Scully R. Mechanisms of double-strand break repair in somatic mammalian cells. Biochem J. 2009; 423:157–168. [PubMed: 19772495]
3. Heller RC, Marians KJ. Replisome assembly and the direct restart of stalled replication forks. Nat Rev Mol Cell Biol. 2006; 7:932–943. [PubMed: 17139333]
4. Petermann E, Helleday T. Pathways of mammalian replication fork restart. Nat Rev Mol Cell Biol. 2010; 11:683–687. [PubMed: 20842177]
5. Nagaraju G, Scully R. Minding the gap: The underground functions of BRCA1 and BRCA2 at stalled replication forks. DNA Repair (Amst). 2007

6. Scully R, Livingston DM. In search of the tumour-suppressor functions of BRCA1 and BRCA2. Nature. 2000; 408:429–432. [PubMed: 11100717]
7. Paques F, Haber JE. Multiple pathways of recombination induced by double-strand breaks in Saccharomyces cerevisiae. Microbiol Mol Biol Rev. 1999; 63:349–404. [PubMed: 10357855]
8. Krogh BO, Symington LS. Recombination proteins in yeast. Annu Rev Genet. 2004; 38:233–271. [PubMed: 15568977]
9. San Filippo J, Sung P, Klein H. Mechanism of eukaryotic homologous recombination. Annu Rev Biochem. 2008; 77:229–257. [PubMed: 18275380]
10. Morrow DM, Connelly C, Hieter P. "Break copy" duplication: a model for chromosome fragment formation in Saccharomyces cerevisiae. Genetics. 1997; 147:371–382. [PubMed: 9335579]
11. Llorente B, Smith CE, Symington LS. Break-induced replication: what is it and what is it for? Cell Cycle. 2008; 7:859–864. [PubMed: 18414031]
12. Kraus E, Leung WY, Haber JE. Break-induced replication: a review and an example in budding yeast. Proc Natl Acad Sci U S A. 2001; 98:8255–8262. [PubMed: 11459961]
13. Malkova A, Haber JE. Mutations arising during repair of chromosome breaks. Annu Rev Genet. 2012; 46:455–473. [PubMed: 23146099]
14. Davis AP, Symington LS. RAD51-dependent break-induced replication in yeast. Mol Cell Biol. 2004; 24:2344–2351. [PubMed: 14993274]
15. Malkova A, Naylor ML, Yamaguchi M, Ira G, Haber JE. RAD51-dependent break-induced replication differs in kinetics and checkpoint responses from RAD51-mediated gene conversion. Mol Cell Biol. 2005; 25:933–944. [PubMed: 15657422]
16. McEachern MJ, Haber JE. Break-Induced Replication and Recombinational Telomere Elongation in Yeast. Annu Rev Biochem. 2006
17. Smith CE, Llorente B, Symington LS. Template switching during break-induced replication. Nature. 2007; 447:102–105. [PubMed: 17410126]
18. Sweetser DB, Hough H, Whelden JF, Arbuckle M, Nickoloff JA. Fine-resolution mapping of spontaneous and double-strand break-induced gene conversion tracts in Saccharomyces cerevisiae reveals reversible mitotic conversion polarity. Mol Cell Biol. 1994; 14:3863–3875. [PubMed: 8196629]
19. Elliott B, Richardson C, Winderbaum J, Nickoloff JA, Jasin M. Gene conversion tracts from double-strand break repair in mammalian cells. Mol Cell Biol. 1998; 18:93–101. [PubMed: 9418857]
20. Taghian DG, Nickoloff JA. Chromosomal double-strand breaks induce gene conversion at high frequency in mammalian cells. Mol Cell Biol. 1997; 17:6386–6393. [PubMed: 9343400]
21. Johnson RD, Jasin M. Sister chromatid gene conversion is a prominent double-strand break repair pathway in mammalian cells. Embo J. 2000; 19:3398–3407. [PubMed: 10880452]
22. Puget N, Knowlton M, Scully R. Molecular analysis of sister chromatid recombination in mammalian cells. DNA Repair (Amst). 2005; 4:149–161. [PubMed: 15590323]
23. Nagaraju G, Odate S, Xie A, Scully R. Differential regulation of short- and long-tract gene conversion between sister chromatids by Rad51C. Mol Cell Biol. 2006; 26:8075–8086. [PubMed: 16954385]
24. Brenneman MA, Wagener BM, Miller CA, Allen C, Nickoloff JA. XRCC3 controls the fidelity of homologous recombination: roles for XRCC3 in late stages of recombination. Mol Cell. 2002; 10:387–395. [PubMed: 12191483]
25. Nagaraju G, Hartlerode A, Kwok A, Chandramouly G, Scully R. XRCC2 and XRCC3 regulate the balance between short- and long-tract gene conversion between sister chromatids. Mol Cell Biol. 2009
26. Saleh-Gohari N, Helleday T. Strand invasion involving short tract gene conversion is specifically suppressed in BRCA2-deficient hamster cells. Oncogene. 2004; 23:9136–9141. [PubMed: 15480413]
27. Tauchi H, et al. Nbs1 is essential for DNA repair by homologous recombination in higher vertebrate cells. Nature. 2002; 420:93–98. [PubMed: 12422221]

28. Sartori AA, et al. Human CtIP promotes DNA end resection. Nature. 2007; 450:509–514. [PubMed: 17965729]
29. Huen MS, Sy SM, Chen J. BRCA1 and its toolbox for the maintenance of genome integrity. Nat Rev Mol Cell Biol. 2010; 11:138–148. [PubMed: 20029420]
30. Greenberg RA. Recognition of DNA double strand breaks by the BRCA1 tumor suppressor network. Chromosoma. 2008; 117:305–317. [PubMed: 18369654]
31. O'Donovan PJ, Livingston DM. BRCA1 and BRCA2: breast/ovarian cancer susceptibility gene products and participants in DNA double-strand break repair. Carcinogenesis. 2010; 31:961–967. [PubMed: 20400477]
32. Hu Y, et al. RAP80-directed tuning of BRCA1 homologous recombination function at ionizing radiation-induced nuclear foci. Genes Dev. 2011; 25:685–700. [PubMed: 21406551]
33. Bunting SF, et al. 53BP1 inhibits homologous recombination in Brca1-deficient cells by blocking resection of DNA breaks. Cell. 2010; 141:243–254. [PubMed: 20362325]
34. Xie A, et al. Control of sister chromatid recombination by histone H2AX. Mol Cell. 2004; 16:1017–1025. [PubMed: 15610743]
35. Jasin M. Genetic manipulation of genomes with rare-cutting endonucleases. Trends Genet. 1996; 12:224–228. [PubMed: 8928227]
36. Shaner NC, et al. Improved monomeric red, orange and yellow fluorescent proteins derived from Discosoma sp. red fluorescent protein. Nat Biotech. 2004; 22:1567–1572.
37. Farmer H, et al. Targeting the DNA repair defect in BRCA mutant cells as a therapeutic strategy. Nature. 2005; 434:917–921. [PubMed: 15829967]
38. Hakem R, et al. The tumor suppressor gene Brca1 is required for embryonic cellular proliferation in the mouse. Cell. 1996; 85:1009–1023. [PubMed: 8674108]
39. Moynahan ME, Chiu JW, Koller BH, Jasin M. Brca1 controls homology-directed DNA repair. Mol Cell. 1999; 4:511–518. [PubMed: 10549283]
40. Chandler J, Hohenstein P, Swing DA, Tessarollo L, Sharan SK. Human BRCA1 gene rescues the embryonic lethality of Brca1 mutant mice. Genesis. 2001; 29:72–77. [PubMed: 11170347]
41. Baer R, Ludwig T. The BRCA1/BARD1 heterodimer, a tumor suppressor complex with ubiquitin E3 ligase activity. Curr Opin Genet Dev. 2002; 12:86–91. [PubMed: 11790560]
42. Drost R, et al. BRCA1 RING function is essential for tumor suppression but dispensable for therapy resistance. Cancer Cell. 2011; 20:797–809. [PubMed: 22172724]
43. Litman R, et al. BACH1 is critical for homologous recombination and appears to be the Fanconi anemia gene product FANCJ. Cancer Cell. 2005; 8:255–265. [PubMed: 16153896]
44. Coleman KA, Greenberg RA. The BRCA1-RAP80 complex regulates DNA repair mechanism utilization by restricting end resection. J Biol Chem. 2011; 286:13669–13680. [PubMed: 21335604]
45. Adamson B, Smogorzewska A, Sigoillot FD, King RW, Elledge SJA. genome-wide homologous recombination screen identifies the RNA-binding protein RBMX as a component of the DNA-damage response. Nat Cell Biol. 2012; 14:318–328. [PubMed: 22344029]
46. Wang B, et al. Abraxas and RAP80 form a BRCA1 protein complex required for the DNA damage response. Science. 2007; 316:1194–1198. [PubMed: 17525340]
47. Kaidi A, Weinert BT, Choudhary C, Jackson SP. Human SIRT6 promotes DNA end resection through CtIP deacetylation. Science. 2010; 329:1348–1353. [PubMed: 20829486]
48. Xie A, et al. Distinct roles of chromatin-associated proteins MDC1 and 53BP1 in mammalian double-strand break repair. Mol Cell. 2007; 28:1045–1057. [PubMed: 18158901]
49. Yun MH, Hiom K. CtIP-BRCA1 modulates the choice of DNA double-strand-break repair pathway throughout the cell cycle. Nature. 2009
50. Westmoreland JW, Resnick MA. Coincident resection at both ends of random, gamma-induced double-strand breaks requires MRX (MRN), Sae2 (Ctp1), and Mre11-nuclease. PLoS Genet. 2013; 9:e1003420. [PubMed: 23555316]
51. Helmink BA, et al. H2AX prevents CtIP-mediated DNA end resection and aberrant repair in G1-phase lymphocytes. Nature. 2011; 469:245–249. [PubMed: 21160476]

52. Jain S, et al. A recombination execution checkpoint regulates the choice of homologous recombination pathway during DNA double-strand break repair. Genes Dev. 2009; 23:291–303. [PubMed: 19204116]

53. Kane DP, Shusterman M, Rong Y, McVey M. Competition between replicative and translesion polymerases during homologous recombination repair in Drosophila. PLoS genetics. 2012; 8:e1002659. [PubMed: 22532806]

54. Lydeard JR, et al. Break-induced replication requires all essential DNA replication factors except those specific for pre-RC assembly. Genes Dev. 2010; 24:1133–1144. [PubMed: 20516198]

55. Ira G, Haber JE. Characterization of RAD51-independent break-induced replication that acts preferentially with short homologous sequences. Mol Cell Biol. 2002; 22:6384–6392. [PubMed: 12192038]

56. Hastings PJ, Ira G, Lupski JRA. microhomology-mediated break-induced replication model for the origin of human copy number variation. PLoS Genet. 2009; 5:e1000327. [PubMed: 19180184]

57. Petermann E, Orta ML, Issaeva N, Schultz N, Helleday T. Hydroxyurea-stalled replication forks become progressively inactivated and require two different RAD51-mediated pathways for restart and repair. Mol Cell. 2010; 37:492–502. [PubMed: 20188668]

58. Hashimoto Y, Puddu F, Costanzo V. RAD51- and MRE11-dependent reassembly of uncoupled CMG helicase complex at collapsed replication forks. Nat Struct Mol Biol. 2012; 19:17–24. [PubMed: 22139015]

59. Stephens PJ, et al. Complex landscapes of somatic rearrangement in human breast cancer genomes. Nature. 2009; 462:1005–1010. [PubMed: 20033038]

60. Scully R, et al. Association of BRCA1 with Rad51 in mitotic and meiotic cells. Cell. 1997; 88:265–275. [PubMed: 9008167]

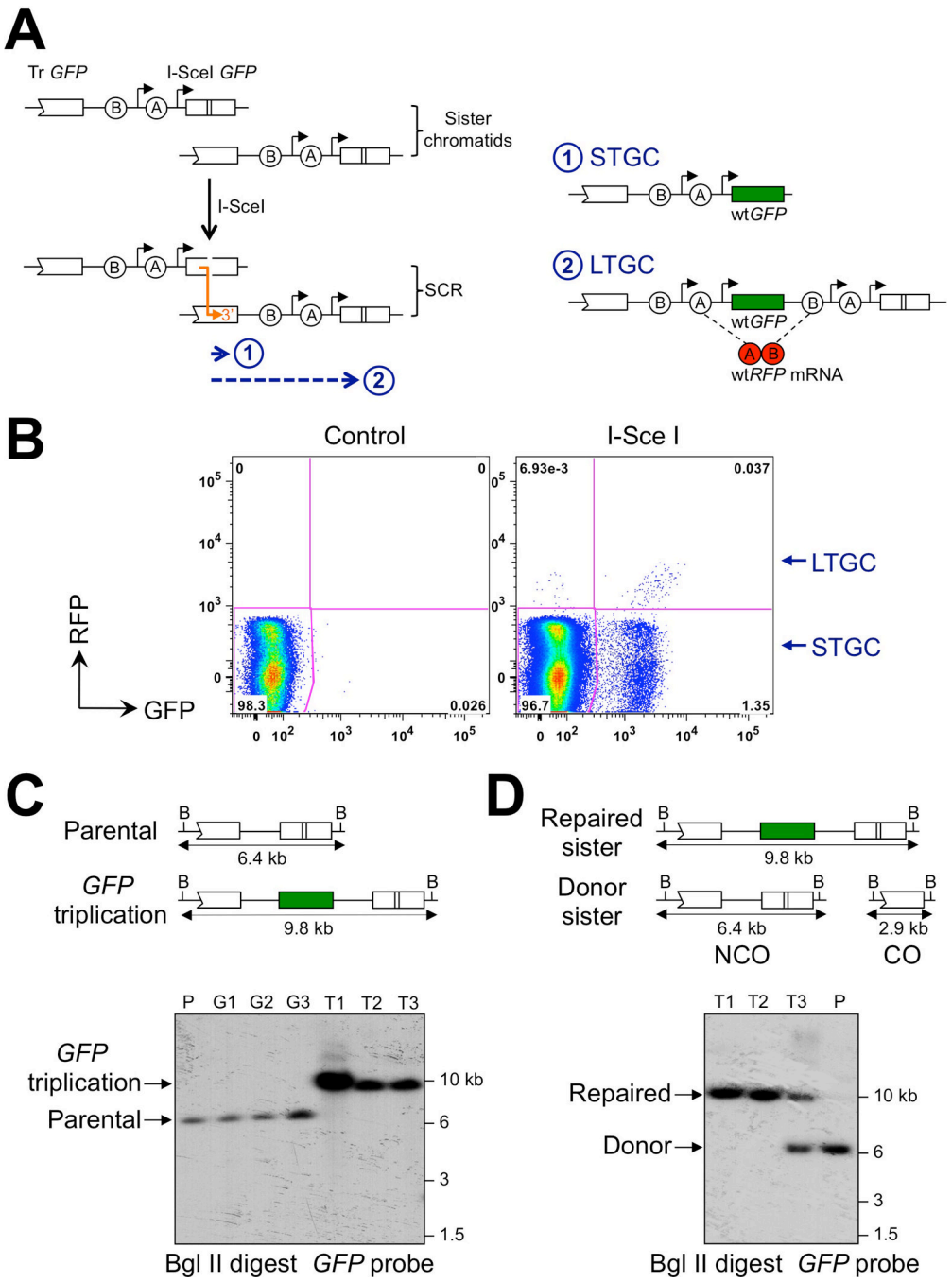


**Figure 1. RFP-SCR reporter for quantifying short tract and long tract gene conversion**

(A) Structure of the RFP-SCR reporter. Circles A and B: 5' and 3' artificial *RFP* exons. Black arrows: promoters. Tr *GFP*: 5' truncated *GFP*. Orange arrow: Rad51-mediated strand invasion (3' end marked with arrow head). Blue dashed arrow #1: short tract gene conversion (STGC); #2: long tract gene conversion (LTGC). LTGC generates wt*RFP* mRNA.

(B) I-SceI-induced HR products in *Brca1*$^{fl/mut}$ RFP-SCR reporter ES cells. Note GFP$^{+}$RFP$^{-}$ (STGC) and GFP$^{+}$RFP$^{+}$ (LTGC) populations.

(C) Southern blot analysis of HR products. "Parental": unrearranged RFP-SCR reporter; "*GFP* triplication": LTGC or crossover product. B: Bgl II sites. Boxes are *GFP* copies; green

box is wt *GFP RFP* cassette is not shown. Gel lanes - P: parental; G1-G3: $GFP^+RFP^-$ STGC products; T1-T3: $GFP^+RFP^+$ "*GFP* triplication" products.
(D) Donor sister chromatid structure distinguishes non-crossover (NCO) from crossover (CO) "*GFP* triplication" outcome. Cartoon elements as in (C). Gel lanes - T1-T3: $GFP^+RFP^+$ clones (different from panel C); P: parental. Note unrearranged donor sister in T3, implying a NCO mechanism (LTGC).

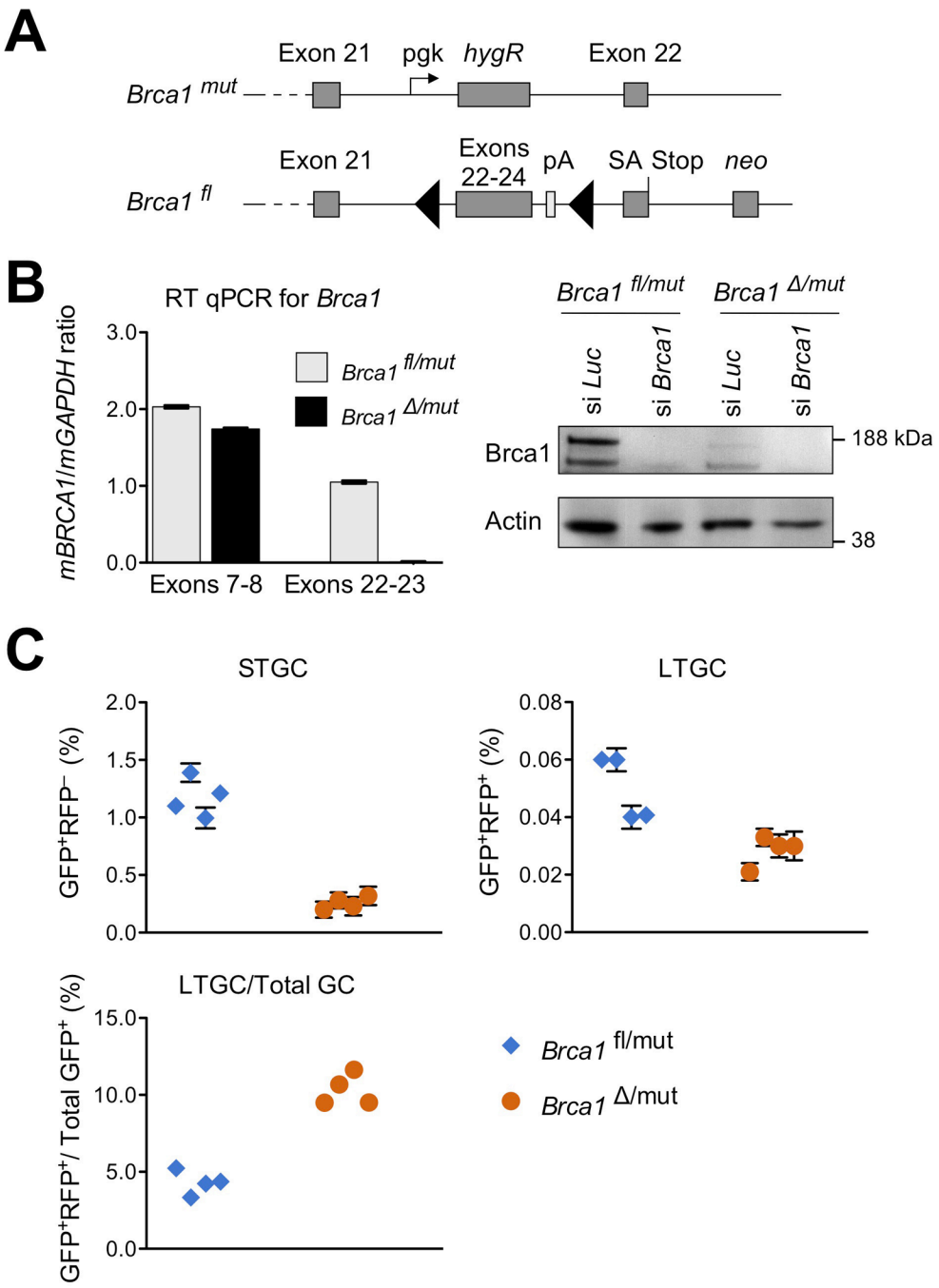


**Figure 2. Bias in favor of LTGC in *Brca1*$^{\Delta/mut}$ ES cells**

(A) *Brca1* gene structure in *Brca1*$^{fl/mut}$ ES cells. *Brca1*$^{mut}$ allele encodes truncated product. *Brca1*$^{fl}$ allele converts to "*Brca1*$^{\Delta}$" following Cre-mediated recombination. Grey boxes: *Brca1* exons; black triangles: *loxP* sites; SA: splice acceptor.

(B) Analysis of *Brca1* gene products in *Brca1*$^{fl/mut}$ and *Brca1*$^{\Delta/mut}$ ES cells. Left panel: RT qPCR analysis of mRNA exon boundaries. Note loss of exon 22-23 signal in *Brca1*$^{\Delta/mut}$ cells. Right panel: Brca1 protein levels in *Brca1*$^{fl/mut}$ and *Brca1*$^{\Delta/mut}$ ES cells following transfection with siRNA against luciferase (si *Luc*) or Brca1 (si *Brca1*). Note persistent Brca1 product in *Brca1*$^{\Delta/mut}$ ES cells, consistent with hypomorphic status.

(C) I-SceI-induced HR in four independent *Brca1*$^{fl/mut}$ (blue diamonds) and four independent *Brca1*$^{\Delta/mut}$ (orange circles) Cre-treated RFP-SCR reporter ES cell clones. Each point shows mean of quadruplicate samples for one independent clone. Error bars: standard error of the mean (SEM) in this and all subsequent figures. STGC, LTGC and LTGC/Total GC products shown. In last panel, error bars were smaller than symbols.

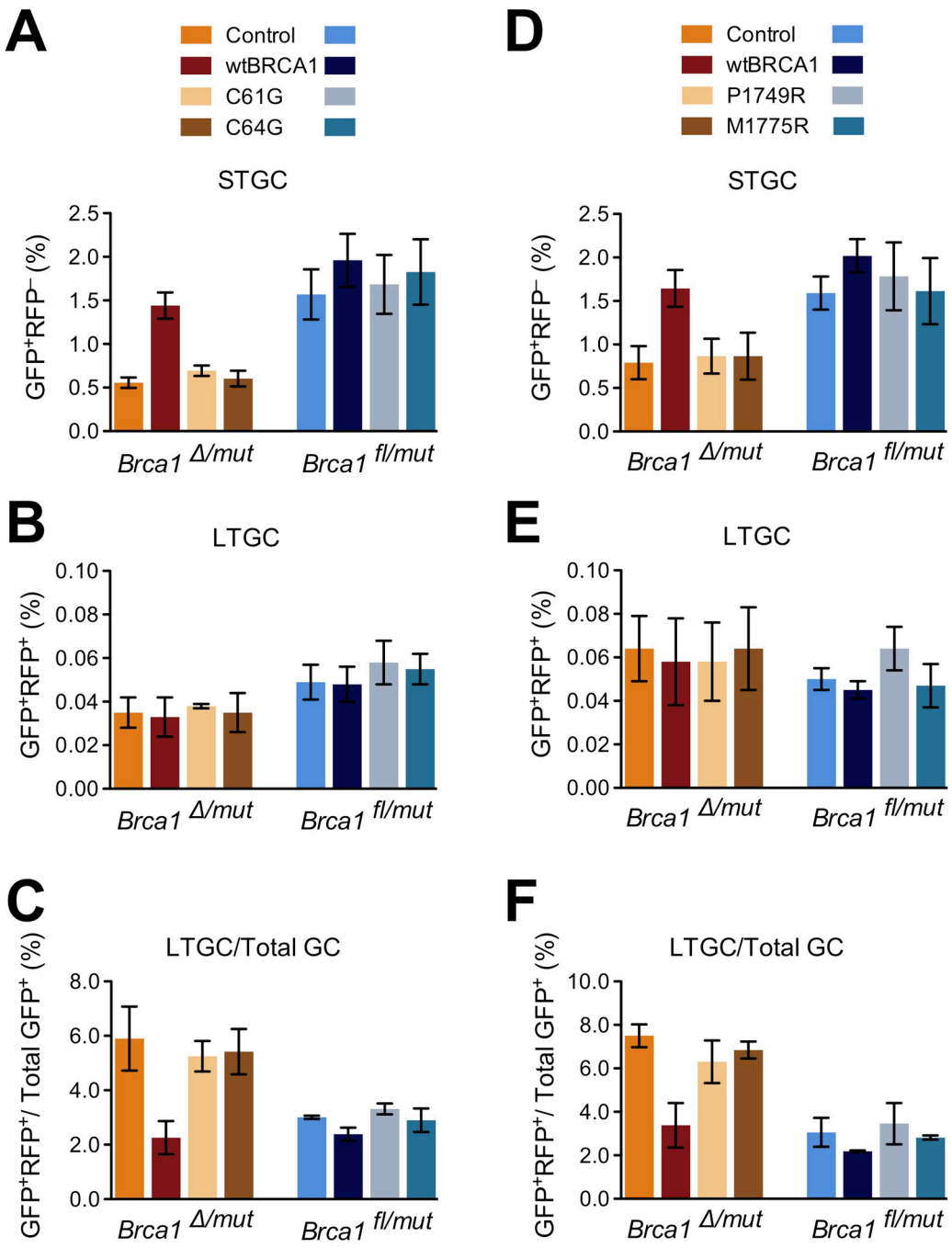


**Figure 3. Wild type but not cancer predisposing mutant alleles of human*BRCA1*complement the STGC defect in*Brca1*$^{\Delta/mut}$ ES cells**

Data pooled from three independent experiments, each performed with triplicate samples. Error bars: SEM, n=3.

(A) I-SceI-induced STGC in *Brca1*$^{\Delta/mut}$ and *Brca1*$^{fl/mut}$ RFP-SCR reporter ES cells transiently transfected with I-SceI and with either control (orange or blue), wt*BRCA1* (maroon or dark blue), *BRCA1* C61G (apricot or grey) or *BRCA1* C64G (brown or teal). *Brca1*$^{\Delta/mut}$ cells: wt*BRCA1 vs.* control: paired *t*-test: P = 0.01. Other *BRCA1* alleles *vs.* control: Not Significant (NS). *Brca1*$^{fl/mut}$ cells: all test samples *vs.* control: NS.

(B) I-SceI-induced LTGC in experiment shown in (A). All test samples *vs.* control: NS.

(C) Ratio of I-SceI-induced LTGC/overall GC in experiment shown in (A) and (B). *Brca1*$^{\Delta/mut}$ cells: wt*BRCA1 vs.* control: paired *t*-test: P = 0.04. Other *BRCA1* alleles *vs.* control: NS. *Brca1*$^{fl/mut}$ cells: all test samples *vs.* control: NS.
(D) Similar to (A), but with *BRCA1* P1749R (apricot or grey) or *BRCA1* M1775R (brown or teal). *Brca1*$^{\Delta/mut}$ cells: wt*BRCA1 vs.* control: paired *t*-test: P = 0.05. Other *BRCA1* alleles *vs.* control: NS. *Brca1*$^{fl/mut}$ cells: all test samples *vs.* control: NS.
(E) I-SceI-induced LTGC events in experiment shown in (D). All test samples *vs.* control: NS.
(F) Ratio of I-SceI-induced LTGC/overall GC in experiment shown in (D) and (E). *Brca1*$^{\Delta/mut}$ cells: wt*BRCA1 vs.* control: paired *t*-test: P = 0.03. Other *BRCA1* alleles *vs.* control: NS. *Brca1*$^{fl/mut}$ cells: all test samples *vs.* control: NS.

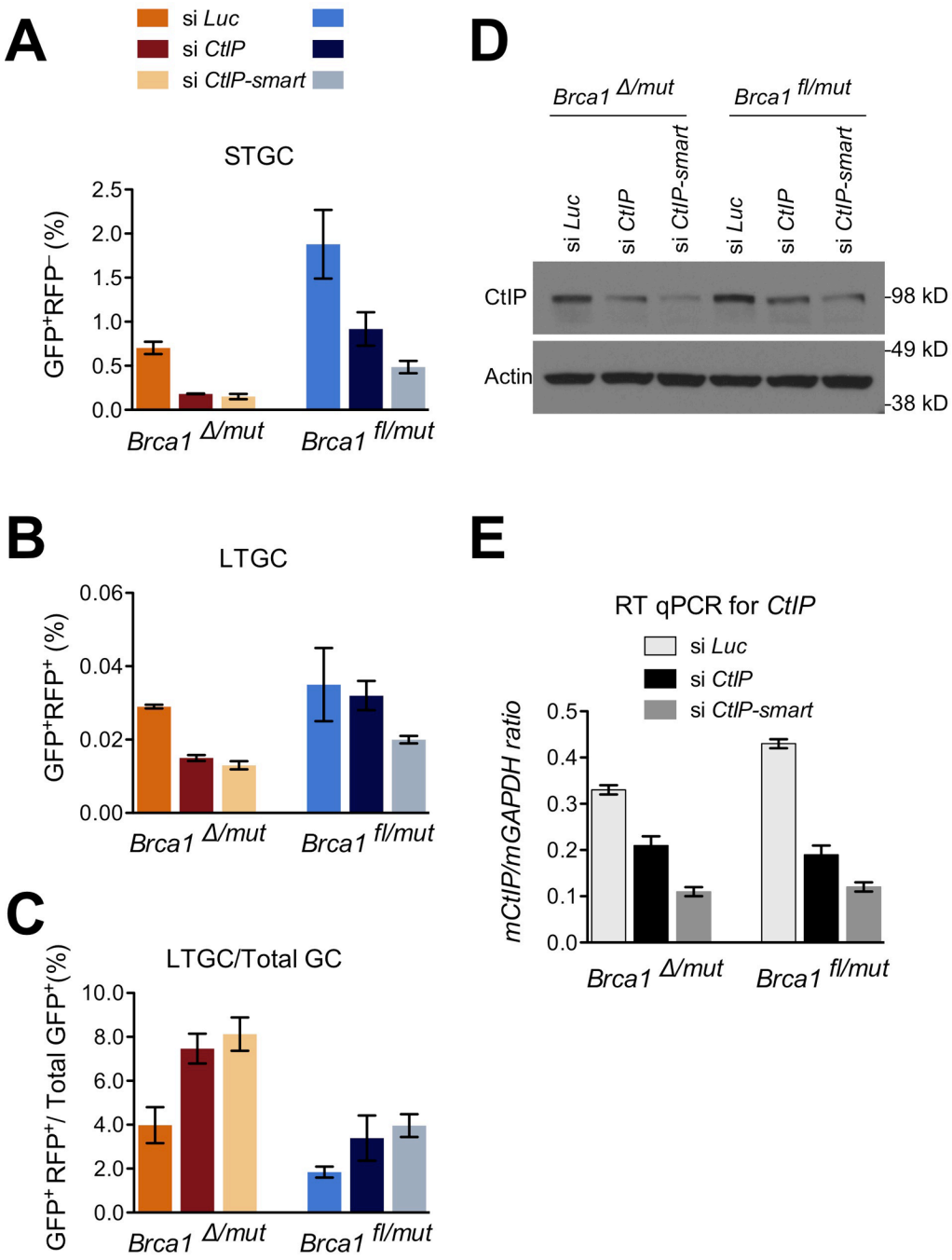


**Figure 4. CtIP controls the balance between LTGC and STGC**

Data pooled from three independent experiments, each performed with triplicate samples. Error bars: SEM, n=3.

(A) I-SceI-induced STGC in *Brca1*$^{\Delta/mut}$ and *Brca1*$^{fl/mut}$ RFP-SCR reporter ES cells co-transfected with I-SceI and with either control Luciferase siRNA (si *Luc*, orange or blue) single CtIP siRNA (si *CtIP*, maroon or dark blue) or CtIP SMARTpool (si *CtIP-smart*, apricot or grey). Paired *t*-test *vs.* si *Luc* in *Brca1*$^{\Delta/mut}$ cells: si *CtIP*: P = 0.03; si *CtIP-smart*: P = 0.03; in *Brca1*$^{fl/mut}$ cells: si *CtIP*: NS. si *CtIP-smart*: P = 0.05.

(B) I-SceI-induced LTGC in experiment shown in (A). Paired *t*-test *vs*. si *Luc* in *Brca1*$^{\Delta/mut}$ cells: si *CtIP*: P = 0.002; si *CtIP-smart*: P = 0.002; in *Brca1*$^{fl/mut}$ cells: si *CtIP*: NS. si *CtIP-smart*: NS.

(C) Ratio of I-SceI-induced LTGC/overall GC in experiment shown in (A) and (B). Paired *t*-test *vs*. si *Luc* in *Brca1*$^{\Delta/mut}$ cells: si *CtIP*: P = 0.04; si *CtIP-smart*: P = 0.04; in *Brca1*$^{fl/mut}$ cells: si *CtIP*: NS. si *CtIP-smart*: P = 0.01.

(D) Abundance of CtIP and actin (loading control) in siRNA-treated cells used in (A), (B) and (C).

(E) RT qPCR analysis of *CtIP* mRNA in siRNA-treated cells used in panels (A), (B) and (C).

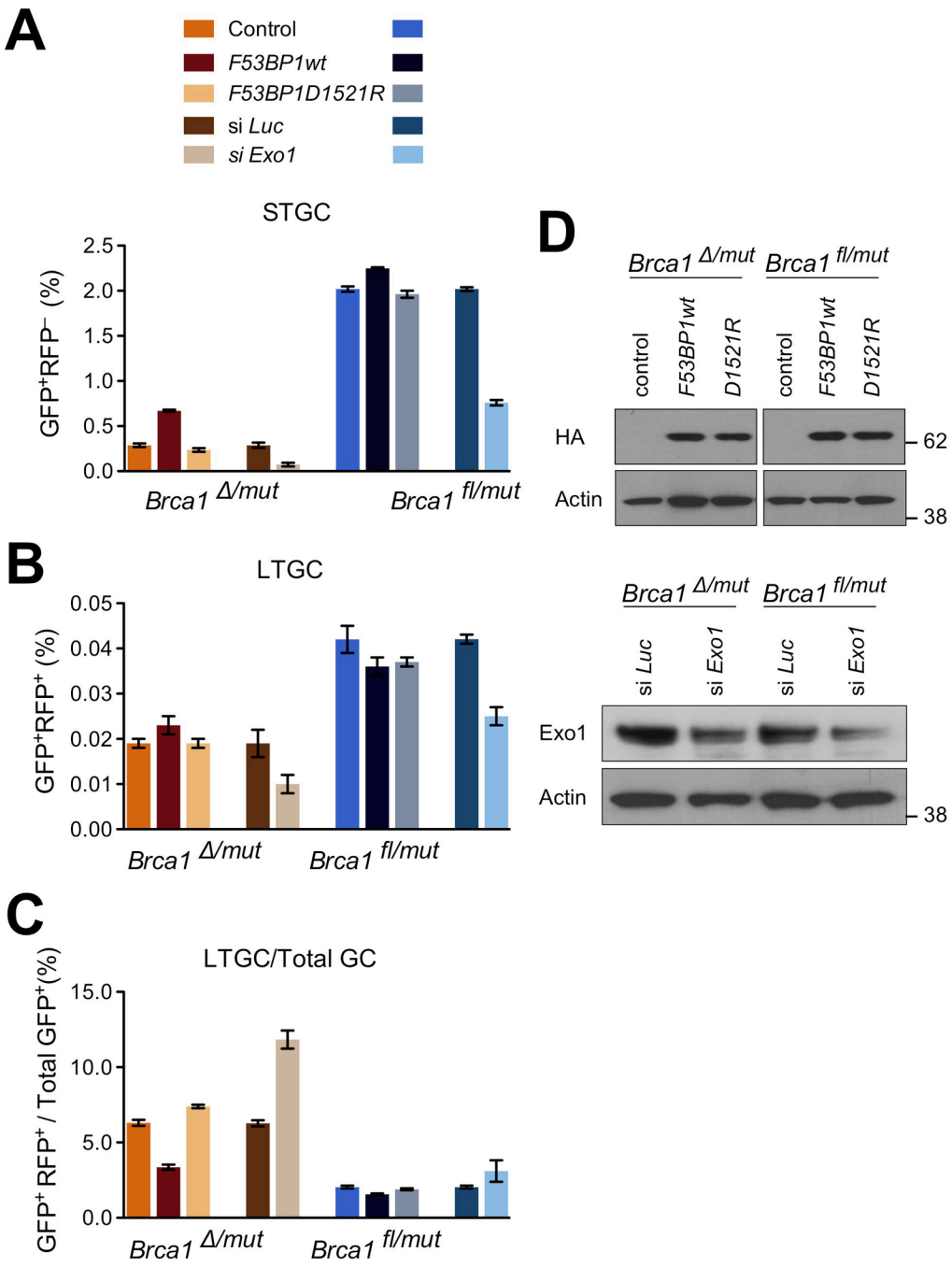


**Figure 5. Impact of overexpression of 53BP1 fragment and siRNA-mediated depletion of Exo1 on STGC and LTGC**

Data pooled from three independent experiments, each performed with triplicate samples. Error bars: SEM, n=3.

(A) I-SceI-induced STGC frequencies in *Brca1*$^{\Delta/mut}$ and *Brca1*$^{fl/mut}$ RFP-SCR reporter ES cells transiently co-transfected with I-SceI expression vector and with either control vector (Control, orange or blue), *F53BP1wt* fragment (*F53BP1wt*, maroon or dark blue), *F53BP1D1521R* fragment (*D1521R*, apricot or grey), Luciferase control siRNA (si *Luc*, brown or teal) or SMARTpool siRNA against *Exo1* (si *Exo1*, light brown or sky blue). Paired *t*-test *vs.* control in *Brca1*$^{\Delta/mut}$ cells: *F53BP1wt*: P = 0.0001: *D1521R*: NS; in

*Brca1*$^{fl/mut}$ cells: *F53BP1wt*: NS, *D1521R*: NS. Paired *t*-test si *Luc vs*. si *Exo1* in *Brca1*$^{\Delta/mut}$ cells: P = 0.00007, in *Brca1*$^{fl/mut}$ cells: P = 0.0001. Error bars indicate SEM throughout.

(B) Frequency of I-SceI-induced LTGC events in the same experiment as panel (A). Paired *t*-test *vs*. control in *Brca1*$^{\Delta/mut}$ cells: *F53BP1wt*: NS: *D1521R*: NS; in *Brca1*$^{fl/mut}$ cells: *F53BP1wt*: NS, *D1521R*: NS. Paired *t*-test si *Luc vs*. si *Exo1* in *Brca1*$^{\Delta/mut}$ cells: P = 0.001, in *Brca1*$^{fl/mut}$ cells: P = 0.007.

(C) Ratio of I-SceI-induced GFP$^{+}$RFP$^{+}$/ total GFP$^{+}$ frequencies (LTGC/ overall GC, expressed as a percentage) from the same experiment as panels (A) and (B). Paired *t*-test against control in *Brca1*$^{\Delta/mut}$ cells: *F53BP1wt*: P = 0.0003, *D1521R*: NS; in *Brca1*$^{fl/mut}$ cells: *F53BP1wt*: NS, *D1521R*: NS. Paired *t*-test si *Luc vs*. si *Exo1* in *Brca1*$^{\Delta/mut}$ cells: P = 0.0001, in *Brca1*$^{fl/mut}$ cells: P = 0.007.

(D) Abundance of 53BP1 fragments, Exo1 and actin (loading control) in treated *Brca1*$^{\Delta/mut}$ and *Brca1*$^{fl/mut}$ RFP-SCR reporter ES cells in (A), (B) and (C).

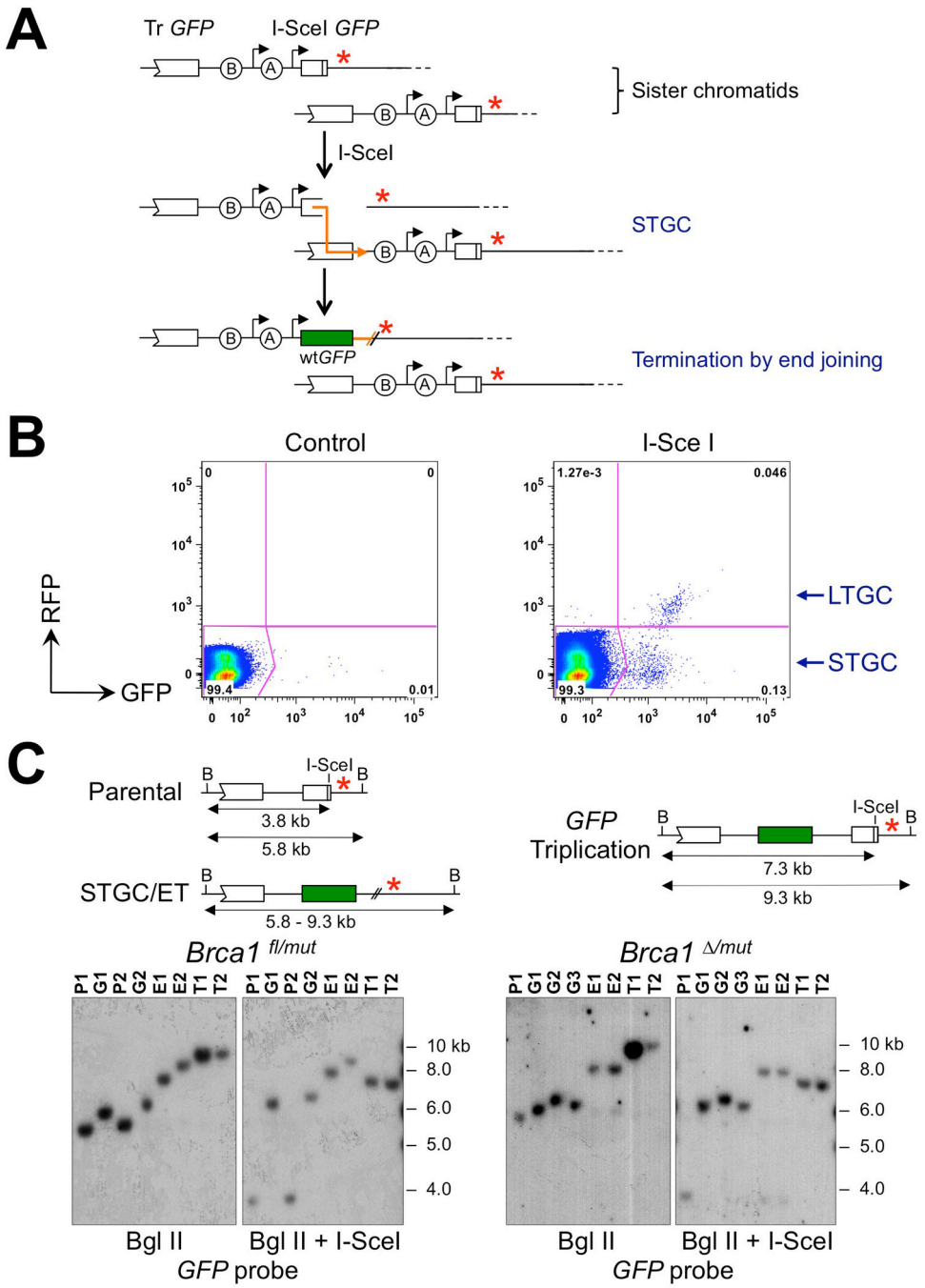


**Figure 6. Analysis of I-SceI-induced STGC and LTGC in "one ended" HR reporter cells**

(A) Structure of the "one-ended" RFP-SCR reporter. Circles A and B: 5' and 3' artificial *RFP* exons. Tr *GFP*: 5' truncated *GFP*. Black arrows: promoters. Orange arrow: Rad51-mediated strand invasion (3' end marked with arrow head). Second (non-invading) end of DSB lacks *GFP* sequences (marked with red star; compare to Figure 1A). Annealing step is not available to terminate STGC ($GFP^+RFP^-$) and STGC termination must occur by end joining. LTGC ($GFP^+RFP^+$) products not shown.

(B) Primary FACS data showing I-SceI-induced HR products in $Brca1^{fl/mut}$ "one ended" RFP-SCR reporter ES cells. Note I-SceI-induced $GFP^+RFP^-$ (STGC) and $GFP^+RFP^+$ (LTGC) populations.

(C) Southern blot analysis of HR products in one-ended RFP-SCR reporter cells. “Parental”: unrearranged reporter; “ET”: “Early termination” LTGC products. For “STGC/ET” events, termination is predicted to occur by end-joining, producing HR products of varying size. “*GFP* triplication”: LTGC product. B: Bgl II sites. I-SceI sites are marked, as are restriction fragment sizes. Boxes are *GFP* copies; green box is wt*GFP RFP* cassette not shown. gDNA from individual clones was digested *in vitro* with BglII alone or with BglII + I-SceI as shown; Southern blot membranes were probed with *GFP* probe. The two left-hand panels (*Brca1*$^{fl/mut}$) are taken from one gel. The two right-hand panels (*Brca1*$^{\Delta/mut}$) are taken from one gel. Gel lanes – P1-P2: parental clones; G1-G3: STGC ($GFP^+RFP^-$) clones; E1-E2: early termination LTGC ($GFP^+RFP^+$) clones; T1-T2: LTGC ($GFP^+RFP^+$) “*GFP* Triplication” clones. Only “parental” and “*GFP* triplication” clones contain an I-SceI site within the repaired reporter; this site is lost in the STGC and ET clones. The slight differences in gel mobility of the G1, G2, E1 and E2 bands between the two panels from the *Brca1*$^{fl/mut}$ gel reflect bowing of the gel during electrophoresis or Southern transfer. Red star: non-homologous second end of I-SceI-induced DSB.

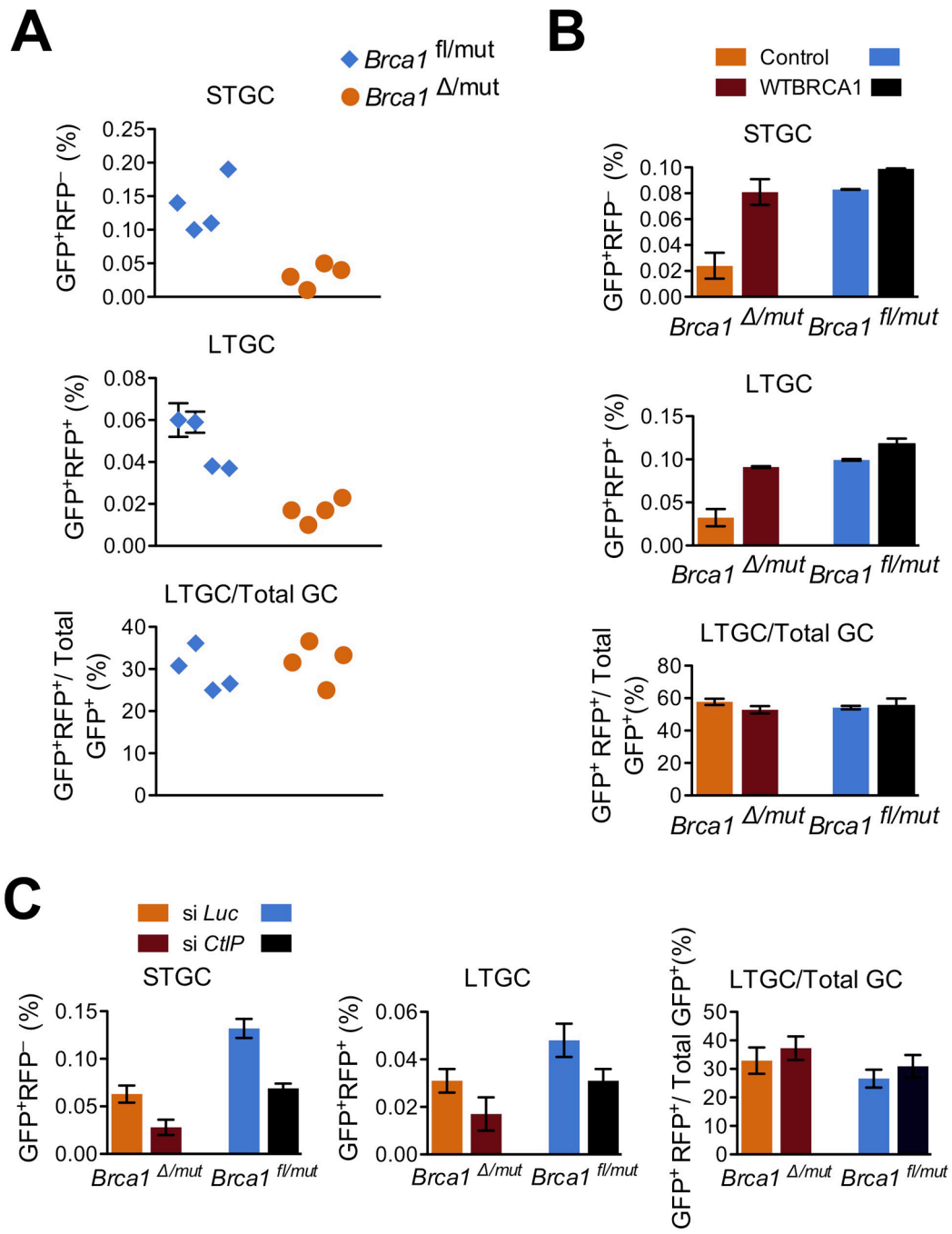


**Figure 7. BRCA1/CtIP fails to affect the STGC/LTGC balance if the annealing step of STGC termination is abolished**

(A) I-SceI-induced HR in four independent Cre-treated one-ended RFP-SCR reporter ES cell clones of each genotype: *Brca1*$^{fl/mut}$ (blue diamonds) and *Brca1*$^{\Delta/mut}$ (orange circles). Each point shows mean of quadruplicate samples for one independent clone. Error bars: standard error of the mean (SEM). If invisible, error bars were smaller than symbols.

(B) Wild type human *BRCA1* complements both the STGC and LTGC defects in *Brca1*$^{\Delta/mut}$ one-ended RFP-SCR reporter ES cells. Data pooled from three independent experiments, each performed in triplicate. Error bars: SEM, n=3.

Top panel: I-SceI induced STGC in *Brca1*$^{\Delta/mut}$ and *Brca1*$^{fl/mut}$ one-ended RFP-SCR reporter ES cells transiently transfected with I-SceI and with either control (orange or blue), or wt*BRCA1* (maroon or dark blue) expression vectors. *Brca1*$^{\Delta/mut}$ cells: wt*BRCA1 vs.* control: paired *t*-test: P = 0.003. *Brca1*$^{fl/mut}$ cells: wt*BRCA1 vs.* control: NS. Middle panel: I-SceI-induced LTGC in experiment shown in top panel. *Brca1*$^{\Delta/mut}$ cells: wt*BRCA1 vs.* control: paired *t*-test: P = 0.003. *Brca1*$^{fl/mut}$ cells: wt*BRCA1 vs.* control: NS. Bottom panel: Ratio of I-SceI-induced LTGC/overall GC in experiment shown in upper panels. *Brca1*$^{\Delta/mut}$ cells: wt*BRCA1 vs.* control: NS. *Brca1*$^{fl/mut}$ cells: wt*BRCA1* vs. control: NS.

(C) CtIP depletion reduces STGC and LTGC in equal proportions in one-ended RFP-SCR reporter cells. Data pooled from three independent experiments, each performed with triplicate samples. Left panel: I-SceI-induced STGC in *Brca1*$^{\Delta/mut}$ and *Brca1*$^{fl/mut}$ RFP-SCR reporter ES cells co-transfected with I-SceI and with either control Luciferase siRNA (si *Luc*, orange or blue bars) or CtIP SMARTpool (si *CtIP*, maroon or dark blue bars). Paired *t*-test in *Brca1*$^{\Delta/mut}$ cells: paired *t*-test: P = 0.05; in *Brca1*$^{fl/mut}$ cells: paired *t*-test: P = 0.02. Middle panel: I-SceI-induced LTGC in same experiment. Paired *t*-test *Brca1*$^{\Delta/mut}$ cells: P = 0.04; in *Brca1*$^{fl/mut}$ cells: NS. Right panel: Ratio of I-SceI-induced LTGC/overall GC in same experiment. Paired *t*-test in *Brca1*$^{\Delta/mut}$ cells: NS; in *Brca1*$^{fl/mut}$ cells: NS.

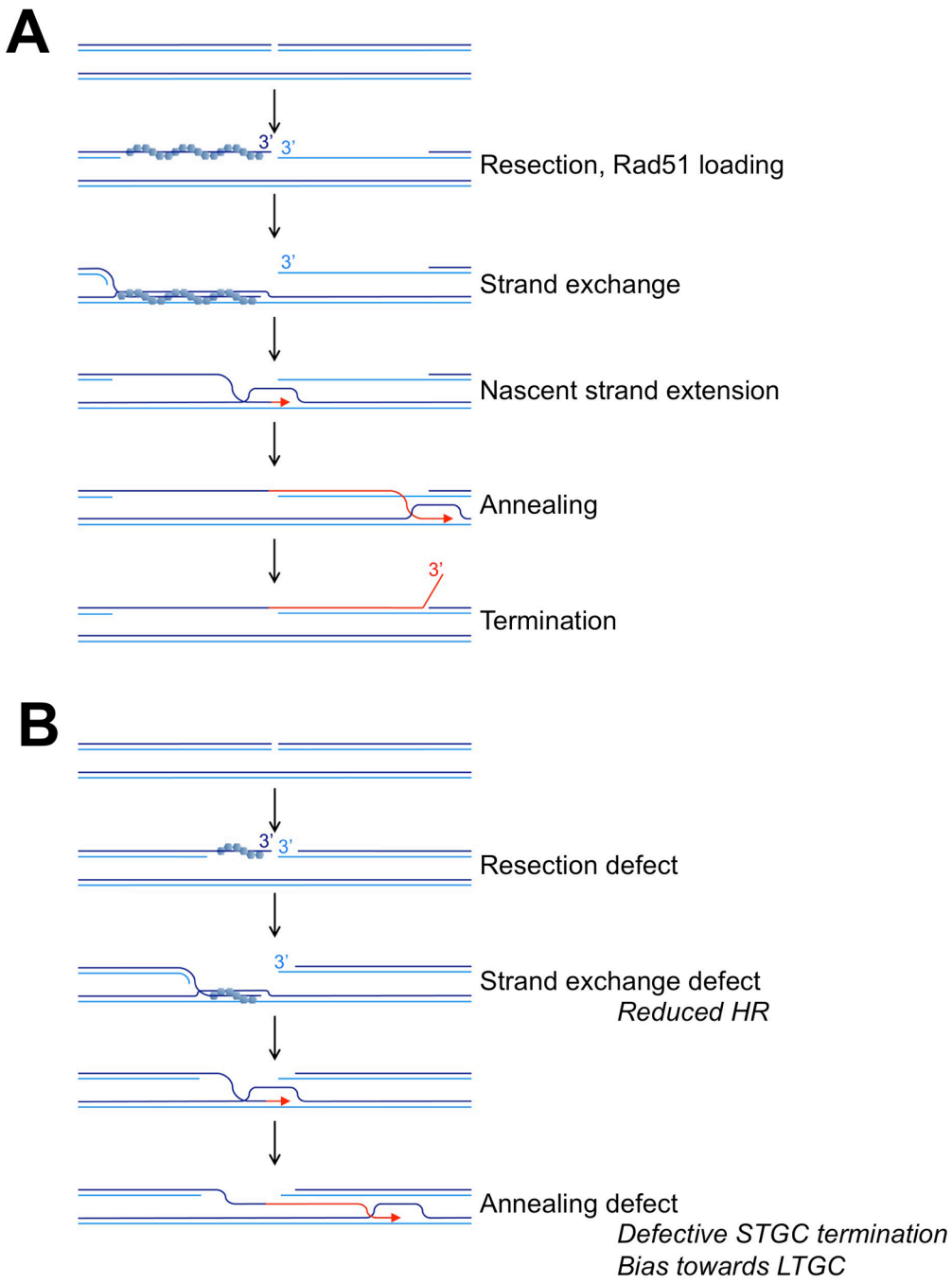


**Figure 8. Model: Brca1/CtIP acts on the second end of the DSB to promote the annealing step of SDSA**

(A) SDSA in wild type cells. Structural analysis of STGC in Figs. 1C and 6C suggest that the homologous second end of the DSB normally "edits" short tract gene conversions to a defined size.

(B) In cells lacking Brca1/CtIP function, defective DNA end resection and impaired cooperation with Brca2/Rad51 results in a strand exchange defect. A defect in second end resection leads to a relative impairment in the annealing step that normally terminates STGC. As a result, a higher proportion of HR events escape termination as STGCs and resolve as LTGCs. In the absence of a homologous second end of the DSB (such as in the

"one-ended" reporter—not shown in this figure), loss of Brca1/CtIP function has no impact on STGC termination and does not affect the STGC/LTGC balance.